Hindawi
Journal of Chemistry
Volume 2023, Article ID 9818621, 1 page
https://doi.org/10.1155/2023/9818621

Retraction

Retracted: Study on Early Warning of Karst Collapse Based on the BP Neural Network

Journal of Chemistry

Received 15 August 2023; Accepted 15 August 2023; Published 16 August 2023

This article has been retracted by Hindawi following an investigation undertaken by the publisher [1]. This investigation has uncovered evidence of one or more of the following indicators of systematic manipulation of the publication process:

(1) Discrepancies in scope
(2) Discrepancies in the description of the research reported
(3) Discrepancies between the availability of data and the research described
(4) Inappropriate citations
(5) Incoherent, meaningless and/or irrelevant content included in the article
(6) Peer-review manipulation

The presence of these indicators undermines our confidence in the integrity of the article's content and we cannot, therefore, vouch for its reliability. Please note that this notice is intended solely to alert readers that the content of this article is unreliable. We have not investigated whether authors were aware of or involved in the systematic manipulation of the publication process.

Wiley and Hindawi regrets that the usual quality checks did not identify these issues before publication and have since put additional measures in place to safeguard research integrity.

We wish to credit our own Research Integrity and Research Publishing teams and anonymous and named external researchers and research integrity experts for contributing to this investigation.

The corresponding author, as the representative of all authors, has been given the opportunity to register their agreement or disagreement to this retraction. We have kept a record of any response received.

References

[1] D. Chen, "Study on Early Warning of Karst Collapse Based on the BP Neural Network," *Journal of Chemistry*, vol. 2022, Article ID 1799772, 7 pages, 2022.

Hindawi
Journal of Chemistry
Volume 2022, Article ID 1799772, 7 pages
https://doi.org/10.1155/2022/1799772

Research Article

Study on Early Warning of Karst Collapse Based on the BP Neural Network

Dongqin Chen

ChangJiang Polytechnic, Wuhan, Hubei 430074, China

Correspondence should be addressed to Dongqin Chen; 31115401@njau.edu.cn

Received 8 June 2022; Revised 30 June 2022; Accepted 8 July 2022; Published 5 August 2022

Academic Editor: K. K. Aruna

In order to comprehensively grasp the dynamics of karst collapse, promote the comprehensive prevention and control level of karst collapse, and prevent secondary disasters caused by lava collapse, this study presents a method of karst collapse early warning based on the BP neural network. This method does not need to set the sliding surface in the finite element calculation model. The stress of the sliding surface is fitted according to the spatial stress relationship of the deep karst layer through the improved BP neural network PID control algorithm and BP neural network algorithm, which avoids the modeling and mesh generation of the complex sliding block and has good accuracy and ease of use. According to the basic theory of the BP neural network, the calculation formulas of multilayer feedforward and error back propagation processes are derived, and the two-dimensional and three-dimensional finite element models of gravity dams without and with sliding blocks are established, respectively. Finally, according to the common formulas of viscoelastic artificial boundary and equivalent load, the two-dimensional and three-dimensional input programs of the karst fluid state are compiled, and a neural network early warning model is obtained. The experimental results show that the process karst state simulated by the algorithm is very close to the actual situation, and the minimum value of antisliding coefficient and its occurrence time can be accurately predicted, with an error range of less than 3%. *Conclusion*. BP neural network prediction can effectively predict karst collapse, with higher prediction accuracy, and can effectively simulate the actual collapse risk.

1. Introduction

The distribution area of karst in China is more than 3.4 million, accounting for about 36% of the land area. Karst area is rich in mineral resources, groundwater, and tourism resources. At the same time, it is also faced with serious geological environment problems such as karst collapse, tunnel water inflow, drought and waterlogging, water and soil pollution, and so on. As one of the most important geological environment problems in the karst area, karst collapse is widely distributed in the world [1]. The formation of karst collapse requires three basic conditions as follows: karst space, a certain thickness of caprock, and trigger factors. Caprock is the main body of collapse. Karst cave gap provides storage and migration space for collapse, which determines the location of collapse to a certain extent, and the trigger factor is the dynamic condition of collapse. There are stress transfer and material transportation among the three, which is comprehensively manifested in the interaction of "rock-soil-water," in which water is of great importance. The changes in groundwater level, velocity, and flow will produce many mechanical effects such as potential corrosion, dissolution, absorption, and water hammer, which will cause the deformation and damage of rock and soil mass and eventually form collapse. In addition to groundwater, gravity and dynamic load are also common factors causing collapse. In recent years, under the double background stress of human engineering activities and extreme climate, karst collapse geological disasters have shown a high-frequency trend, and their spatial and temporal distribution, loss degree, depth, and breadth of impact have also undergone new changes. The concealment, abruptness, repetition, and unpredictability are becoming increasingly prominent [2]. Throughout the study of karst collapse, the

five in one technical and theoretical framework system of "genetic mechanism, identification and evaluation, monitoring and alarm, emergency response and risk management" has been formed. So far, however, the problem of "where, when, and how to collapse" has not been well solved [3]. The prevention and control of karst collapse is still a world-class technical problem in the field of geoscience, which is mainly reflected in the insufficient quantification of the genetic mechanism and the identification and evaluation method of hidden dangers. That is to say, the early warning mechanism and algorithm are still imperfect.

Therefore, the combination of the BP neural network algorithm can avoid the modeling of the sliding block. Only the coordinate information of the sliding surface can be extracted to fit the internal stress value of the karst, which greatly reduces the workload of fluid calculation. It can more effectively monitor the risk of lava and give early warning.

2. Literature Review

For the research on early warning of karst collapse, Wang et al. and others proposed to combine the characteristics of biological neurons receiving and transmitting signals and put forward the mathematical model MP model of neurons, creating a new era of human research on neural networks. The change of connection strength between neurons is analyzed, and the idea of the neural network learning Hebb learning rule is proposed [4]. Zhao et al. and others proposed a learning algorithm that can simulate the human learning process, which is called perceptron, which means that the neural network has the learning ability [5]. Abdelfatah and others put forward the Hopfield network model, which makes the research of the neural network enter the next stage of development. This is a single-layer interconnection. The improved backpropagation algorithm is introduced into the multilayer perceptron, and the BP neural network learning algorithm is proposed. The research on the neural network has become a hot spot again [6]. Chen et al. and others put forward the analysis of the performance of the BP neural network nonlinear function and proved that the feedforward neural network with only one hidden layer and any continuous S-type nonlinear function can approximate any complex function [7]. Mahmoudabadbozchelou et al. and others put forward the Delphi method for quantification and conducted the empirical analysis. It can be seen that the fuzzy neural network model has advantages in coal mine safety evaluation. The fuzzy neural network model combined with fuzzy theory and neural network technology not only has the ability of learning, connection, and adaptation but also has fuzzy thinking, which can make the evaluation results more objective [8]. Mazzi et al. and others put forward the coal mine safety early warning evaluation method based on a neural network and genetic algorithm. The neural network has good self-learning, adaptive, parallel processing, and nonlinear computing capabilities, so it has been widely used in intelligent control, nonlinear optimization, signal processing, and other aspects [9]. Yilmaz and Koyuncu others proposed a genetic algorithm to optimize neural network weights and thresholds to establish a coal mine accident prediction model [10]. They found that compared with the traditional algorithm, it has better prediction accuracy and faster convergence speed. They concluded that a genetic algorithm to optimize the neural network is feasible and effective.

In this study, the BP neural network algorithm can avoid the modeling of the sliding block. Only the coordinate information of the sliding surface can be extracted to fit the stress value in the karst, which greatly reduces the workload of fluid calculation. In this study, the improved BP neural network PID control algorithm is used to simulate, so as to monitor and warn the lava quickly and effectively.

3. Research Methods

3.1. Karst Collapse Hidden Danger Identification and Evaluation System and Data Acquisition. The identification of hidden danger of karst collapse is generally divided into two scales as follows: regional scale and site scale. On the regional scale, with the continuous improvement of the resolution of satellite images and the development of new aviation technologies such as laser radar and synthetic aperture radar, remote sensing has become a major technical method. It has the advantages of wide coverage and rapid identification in the investigation and description of the status quo of collapse pits and the comparative analysis of development trends. At the site scale, geophysical prospecting is a common and effective technical means. In recent years, with the development of electrical seismic and other joint geophysical exploration technologies, the accuracy and depth of karst collapse detection have been significantly improved. For example, the comprehensive application of different methods such as ground geological radar, resistivity imaging, seismic refraction, and microgravity has effectively solved the problem of detection at different depths. At the same time, the application of cross-hole CT, borehole radar, and other technical methods has also effectively solved the problem of precision depiction from coarse to fine. The evaluation of karst collapse can be divided into three levels as follows: susceptibility, risk, and risk. Susceptibility assessment is to evaluate the geological background of karst collapse. Risk assessment is to study the stability of karst collapse under the action of trigger factors on the basis of susceptibility assessment. Risk assessment needs to comprehensively consider the risk and risk of loss of personnel and property. For the evaluation of karst collapse, the key is to establish an evaluation model and determine the weights and interrelations of various factors. Commonly used methods include decision tree, stepwise regression analysis, AHP, fuzzy mathematics, and neural network. Different methods have their own advantages and disadvantages. The accuracy depends critically on the knowledge and quantification of the genetic mechanism of karst collapse. The most important data to be obtained mainly includes the following four aspects: first, karst collapse triggered by subgrade and underground space engineering; second, the rapid change of hydrodynamic conditions has seriously damaged the equilibrium state of rock and soil mass and induced karst collapse. The main reasons for the sharp change in

hydrodynamic conditions are rainfall, reservoir water storage, underground water filling, irrigation leakage, serious drought, underground drainage, and high-intensity pumping; third, additional load; and fourth, acid-based solution corrosion caused by waste liquid [11].

3.2. BP Neural Network Structure. The structure of the BP neural network is shown in Figure 1. It uses a three-layer structure of output layer, hidden layer, an input layer, and *j*, *i*, and *l* represent the input layer node, the hidden layer node, and the output layer nodes, respectively. The number of input nodes in the input layer is 4, the number of hidden nodes in the hidden layer is 5, and the number of output nodes in the output layer is 3. The input node corresponds to the system's expected value, actual value, deviation, and control size, and the output layer node corresponds to the parameters K_p, K_i, and K_d, one by one, of the PID control algorithm (Figure 1).

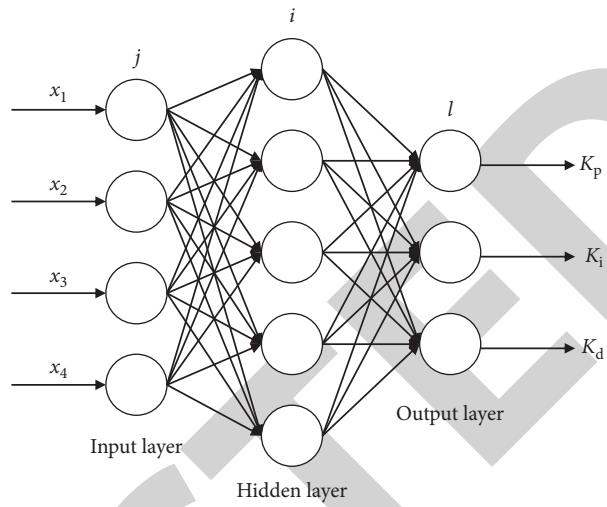

Figure 1: BP neural network structure.

The BP (back-propagation) neural network is one of the many artificial neural networks that the teacher learns, usually consisting of a data input layer, a hidden layer of nonlinear activation function, a linear output layer, and a BP neural network. The structure of the model is shown in Figure 1 [12]. The first is the forward multilayer feedforward process: the network randomly assigns the initial connection weight and threshold (also known as deviation) to each neuron according to the number of hidden layers and hidden layer units set by the user. The input layer data are processed by linear weighing of the net input of the latent layer, the weight, and the threshold. Output layer input: after the linear conversion of weight and threshold from layer to layer, the output layer results in a nonlinear activation function of neurons in the output layer. Then, there is the process of error redistribution: the loss function is used to calculate the total error between the output layer result and the expected output result, and then according to different optimization algorithms, the loss function is used to calculate the partial derivatives of the neurons, weights, and other parameters of each layer, so as to obtain the parameter update direction to reduce the error. Set the descent step size and repeatedly adjust the error of the weight and threshold, so that the error is continuously reduced until it reaches an acceptable level or the preset learning times [13]. The algorithm of the BP neural network is shown in Figure 2.

BP neural networks are often used to address adjustment and classification problems. Depending on the complexity of the problem, the number of latent layers, the number of neurons in each layer, and the activation function of the neurons in each layer can be flexibly adjusted.

3.3. Sample Data Division and Learning Rate. To prevent overconfiguration of the neural network by relying too much on the training package data, we divide the sample input data into training packages, validation packages, and test packages, and the validation packages and test packages are not included in the training packages neural network. When the neural network updates the parameters such as weight and deviation for each iteration of the training set data, it checks the verification set error under the current parameters [14]. As the neural network continuously reduces the error of the training set through multiple iterations, it is prone to overfitting. At this time, the error of the verification set will increase with the occurrence of overfitting. When the error of the verification set does not continue to decrease after multiple iterations, the neural network will stop training in advance and save the weight and deviation before the error increases as the optimal network parameters [15]. There are two main functions of the test set. On the one hand, the test set can be used to evaluate the generalization ability of the neural network after the training. On the other hand, it can indicate whether the division of the dataset is reasonable to a certain extent according to whether the number of iterations required for the test set to reach the minimum value is roughly the same as that required for the verification set to reach the minimum value [16].

The methods of dividing training, verification, and test sets generally include random data division, continuous data division, staggered selection of data division, according to index [17]. This study uses the method of randomly dividing data to further strengthen the disorder of the training set and improve the generalization ability of the network. In the follow-up training process, it can be seen that the number of iterations when the error of the validation set and the test set reaches the minimum value is the same, indicating that the method of randomly dividing data is reasonable [18, 19].

In practical application, it is difficult to quickly determine the optimal learning rate. With the development of the BP neural network, the learning rate is no longer a fixed value. The generation of variable learning rate overcomes the traditional disadvantage of difficulty to determine the initial learning rate, speeds up the search speed, effectively improves the accuracy of the results, and also solves the oscillation phenomenon in the later stage of network training [20]. The commonly used learning rate setting method is the exponential decay learning rate method, that is, the learning rate is large at the initial stage of training, and the learning rate decreases continuously with the progress of training until the model converges.

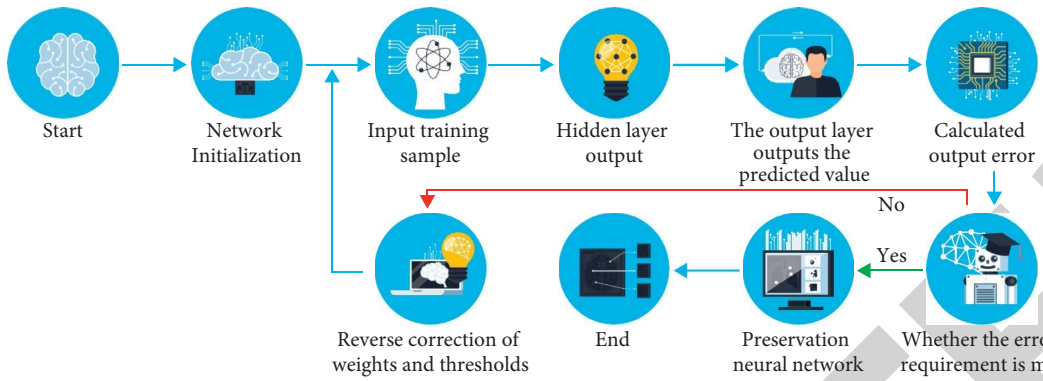

Figure 2: Flowchart of the BP neural network algorithm.

3.4. BP Neural Network PID Controller. The BP neural network unit and PID controller unit are combined to form a BP neural network PID controller. Its principle is that the BP neural network outputs the optimal PID control parameters through self-learning and weight coefficient adjustment according to the current operating state of the system, so that the three adjustable parameters of the PID controller can adapt to changes. Its structure is shown in Figure 3.

The input quantity of the BP neural network input layer is shown in the following formula:

$$o_j^{(1)} = x(j), \quad j = 1, 2, 3, 4. \tag{1}$$

The input and output quantities of the BP neural network hidden layer are, respectively, shown in the following formulas:

$$\text{net}_i^{(2)}(k) = \sum_{j=0}^{m} w_{ij}^{(2)} O_j^{(1)}(k), \tag{2}$$

$$o_i^{(2)}(k) = f\left[\text{net}_i^{(2)}(k)\right], \quad i = 1, 2, \ldots, 5. \tag{3}$$

The hyperbolic tangent function is used as the excitation function of hidden layer neurons, as shown in the following formula:

$$f(x) = \frac{e^x - e^{-x}}{e^x + e^{-x}}. \tag{4}$$

The input and output quantities of the BP neural network output layer are, respectively, shown in the following formulas:

$$\text{net}_i^{(3)}(k) = \sum_{i=0}^{q} w_{li}^{(3)} O_i^{(2)}(k), \tag{5}$$

$$o_l^{(3)}(k) = g\left(\text{net}_l^{(3)}(k)\right). \tag{6}$$

It is obtained from the following formula:

$$\begin{aligned} o_1^{(3)}(K) &= K_p, \\ o_2^{(3)}(K) &= K_i, \\ o_3^{(3)}(K) &= K_d, \end{aligned} \tag{7}$$

where $\omega_{li}^{(3)}$ is the weighting coefficient from hidden layer to output layer; $g(x)$ is the activation function of neurons in the output layer, expressed in the following formula:

$$g(x) = \frac{1 + \tanh(x)}{2} = \frac{e^x}{e^x + e^{-x}}. \tag{8}$$

The performance index function is

$$E(k) = \frac{1}{2}[r(k+1) - y(k+1)]^2. \tag{9}$$

In order to speed up the convergence, an inertia term is added to make the search converge to the global minimum quickly. The formula of the neural network weight coefficient is modified according to the gradient descent method, as shown in the following formula.

$$\Delta\omega_{li}^{(3)}(k+1) = -\eta \frac{\partial E(k)}{\partial \omega_{li}^{(3)}} + \alpha \Delta\omega_{li}^{(3)}(k), \tag{10}$$

where η is the learning rate; α is the momentum factor. The following equation can be obtained from equation (7).

$$\begin{cases} \dfrac{\partial u(k)}{\partial o_1^{(3)}(k)} = e(k) - e(k-1), \\ \dfrac{\partial u(k)}{\partial o_2^{(3)}(k)} = e(k), \\ \dfrac{\partial u(k)}{\partial o_3^{(3)}(k)} = e(k) - 2e(k-1) + e(k-2). \end{cases} \tag{11}$$

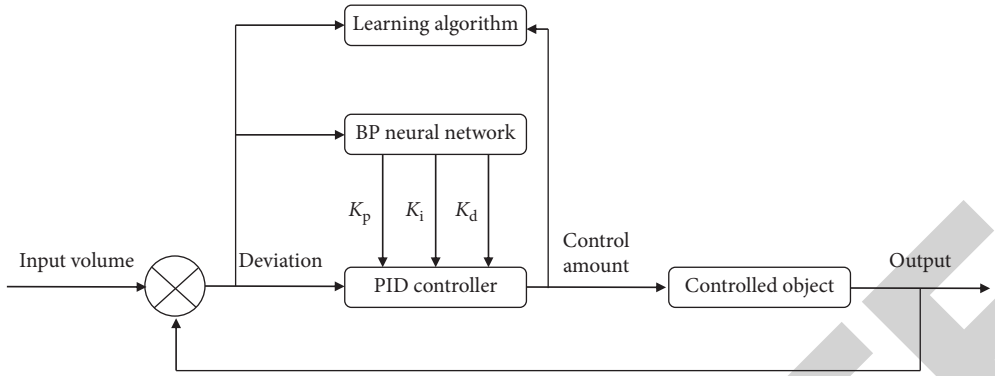

Figure 3: Structure of the BP neural network PID controller.

Thus, the output layer weight calculation formula of the BP neural network can be obtained as

$$\Delta\omega_{li}^{(3)}(k+1) = \eta e(k+1)\operatorname{sgn}\left(\frac{\partial y(k+1)}{\partial u(k)}\right) \frac{\partial u(k)}{\partial o_l^{(3)}(k)} g\left[\operatorname{net}_l^{(3)}(k)\right] o_j^{(2)}(k) + \alpha\Delta\omega_{li}^{(3)}k,$$
$$j = 1, 2, 3, 4,$$
$$i = 1, 2, 3. \tag{12}$$

Calculation formula of the classical incremental PID controller is

$$\mu(k) = \mu(k-1) + K_p[e(k) - e(k-1)] + K_i e(k) + K_d[e(k) - 2e(k-1) + e(k-2)], \tag{13}$$
$$e(k) = r(k) - y(k),$$

where K_p, K_i, and K_d are the proportional, integral, and differential coefficients of PID controller, respectively; $\mu(k)$ is the output of the PID controller; $y(k)$ is the actual output value of the controlled object; $r(k)$ is the expected value of the system; $e(k)$ is the system deviation [21].

3.5. Improved BP Neural Network PID Control Algorithm. The rate of learning remains the same during the study of traditional BP neural networks. If the rate of learning is too high, increasing the weight will cause the network to fluctuate with minimal error and make it impossible to integrate the network.

In order to improve the performance of the BP neural network, the term impulse was added and improved in this study. The function of the torque term is to remember the direction of change in the weight of the connection at the last moment. Increasing the momentum term can obtain a larger learning rate coefficient and improve the learning speed. The oscillation phenomenon may occur in the training process of the neural network, and the "inertia effect" of the momentum term can inhibit the oscillation and buffer. The correction of weight is

$$\Delta\omega(n) = -\eta\frac{\partial E_{(n)}}{\partial_\omega} + \alpha_1\Delta\omega(n-1). \tag{14}$$

Combining the above improved BP neural network with a PID controller, a new BP neural network PID controller (NBPPID) was created, the structure of which is shown in Figure 4.

The steps of the improved algorithm are as follows:

(1) Determine the structure of the BP neural network, initialize the weight coefficients of the input layer, hidden layer, and output layer of the BP neural network, and select appropriate momentum factors α_1, α_2 and learning rate η to make $k = 1$;

(2) The input and output are obtained by sampling, and the deviation is calculated;

(3) The inputs and outputs of the neurons in the input layer, hidden layer, and output layer of the BP neural network are determined. The control parameters K_p, K_i, and K_d of the PID controller are determined by the outputs of the output layer;

(4) PID controller outputs control quantity

(5) The BP neural network adaptively adjusts PID control parameters by adjusting weighting coefficients online

(6) Let $k = 1$ and return to step 1

4. Result Analysis

The improved monitoring algorithm (NBPPID) was compared with the traditional BP neural network PID control algorithm (BPPID) and BP neural network PID control algorithm (MBPPID) through the performance of the improved BP neural network PID control algorithm. The simulation experiment is carried out with MATLAB, and the time-varying nonlinear simulation system is taken as

$$y(k) = \frac{\alpha(k)y(k-1)}{1 + y^2(k-1)} + \mu(k-1), \tag{15}$$

where $\alpha(k) = 1.3(1 - 0.6e^{-0.2k})$.

The structure adopted by the BP neural network has a learning rate of $\eta = 0.2$, $\alpha_1 = 0.5$, $\alpha_2 = 0.1$. Compared with

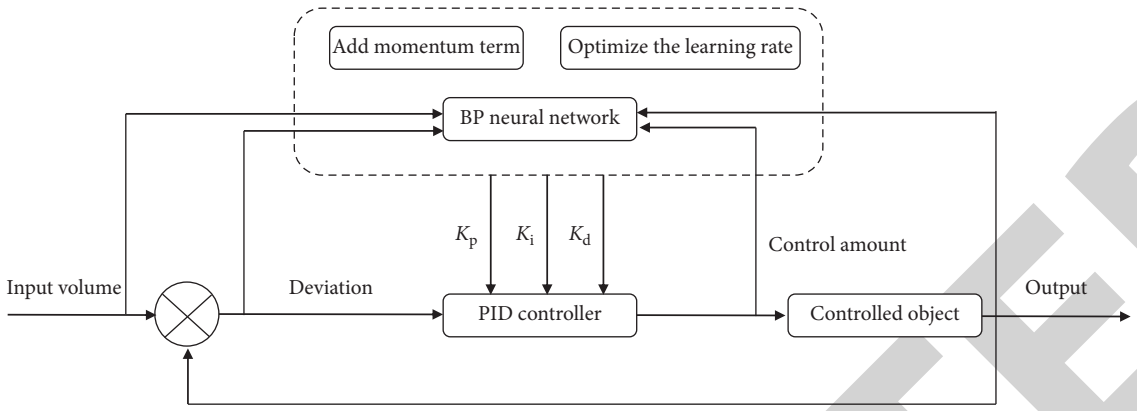

Figure 4: Improved BP neural network PID controller structure.

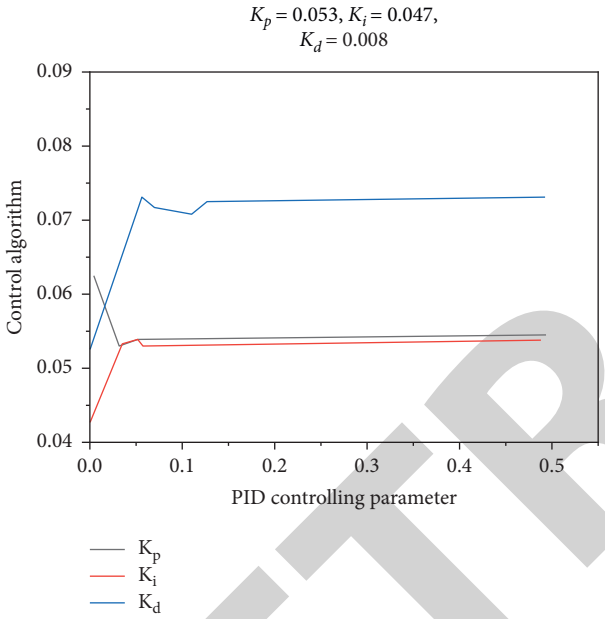

Figure 5: PID control parameter curve of three control algorithms.

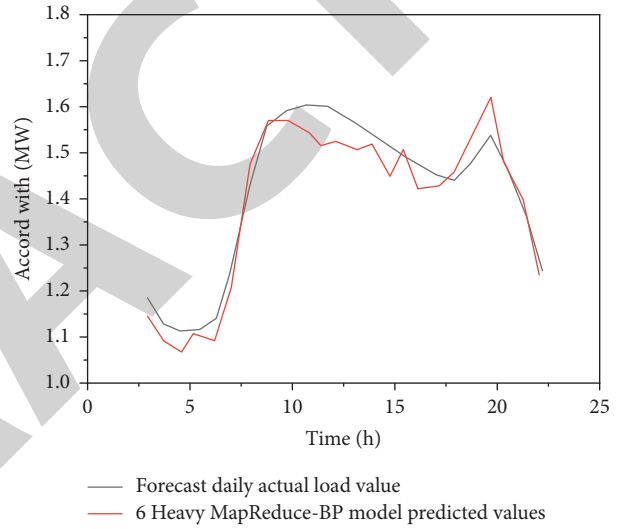

Figure 6: Load forecasting results of the neural network.

the traditional BP neural network PID control algorithm, NBPPID and MBPPID algorithms can effectively alleviate the oscillation phenomenon, and NBPPID reaches the expected value before the MBPPID algorithm, which speeds up the convergence speed. Figure 5 shows the control parameter curves of three control algorithms PID. It can be seen from Figure 5 that the optimal value of PID control parameters of the NBPPID control algorithm is as follows:

$$\begin{aligned} K_p &= 0.053, \\ K_i &= 0.047, \\ K_d &= 0.008. \end{aligned} \tag{16}$$

By improving the learning rate and momentum factor, the algorithm uses the momentum factor to optimize the learning rate and increase the momentum term to suppress the possible oscillation in network training. In the control process, the NBPPID control algorithm adaptively adjusts PID parameters. Input the monitoring data into the BP neural network to obtain the corresponding curve, as shown in Figure 6.

5. Conclusion

Experimental results show that the PID neural network algorithm can effectively alleviate the phenomenon of fluctuations and accelerate the integration rate of the algorithm. When using the BP neural network method to calculate deep melting stability, regression coefficient, and mean squared error, it is not possible to determine the effective force and slip protection coefficient of the sliding surface, used as a measuring neural network. Compared with the antisliding coefficient calculated by the sliding block model, this index can represent the error level between the predicted value and the accurate value of the ground subsidence coefficient. Compared with the preset sliding surface model, the neural network repeated the prediction scheme 12 times, and taking the mean value at each time can be used as the final early warning result, and the karst state in the whole experimental simulation process is very close to the actual situation. The minimum value of antisliding coefficient and its occurrence time can be accurately predicted, and the error range is within 3%. It also shows that the BP neural network is very accurate in the early warning of karst collapse and can effectively simulate the actual collapse risk.

Data Availability

The data used to support the findings of this study are available from the corresponding author upon request.

Conflicts of Interest

The author declares that there are no conflicts of interest.

Acknowledgments

This study was supported by the Construction Science and Technology Project of Hubei Province, Department of Housing and Urban-Rural Development of Hubei Province (2021, number 2075).

References

[1] G. Jin, M. Wang, J. Zhang, H. Sha, and J. Huang, "Stgnn-tte: travel time estimation via spatial–temporal graph neural network," *Future Generation Computer Systems*, vol. 126, pp. 70–81, 2022.

[2] S. Gadde, A. S. N. Charkravarthy, S. Satyanarayana, and M. Murali, "Automatic identification of drug sensitivity of cancer cell with novel regression-based ensemble convolution neural network model," *Soft Computing*, vol. 26, no. 11, pp. 5399–5408, 2022.

[3] R. Shanker and M. Bhattacharya, "Classification of brain mr images using modified version of simplified pulse-coupled neural network and linear programming twin support vector machines," *The Journal of Supercomputing*, vol. 78, no. 11, pp. 13831–13863, 2022.

[4] X. Wang, D. Ding, H. Dong, and X. M. Zhang, "Neural-network-based control for discrete-time nonlinear systems with input saturation under stochastic communication protocol," *IEEE/CAA Journal of Automatica Sinica*, vol. 8, no. 4, pp. 766–778, 2021.

[5] N. Zhao, H. Gao, X. Wen, and H. Li, "Combination of convolutional neural network and gated recurrent unit for aspect-based sentiment analysis," *IEEE Access*, vol. 9, pp. 15561–15569, 2021.

[6] M. A. Abdelfatah, "Artificial neural network for improving the estimation of weighted mean temperature in Egypt," *Journal of Applied Geodesy*, vol. 16, no. 1, pp. 59–64, 2022.

[7] L. Chen, H. Xiong, X. Sang, C. Yuan, X. Li, and Q. Kong, "An innovative deep neural network–based approach for internal cavity detection of timber columns using percussion sound," *Structural Health Monitoring*, vol. 21, no. 3, pp. 1251–1265, 2022.

[8] M. Mahmoudabadbozchelou, M. Caggioni, S. Shahsavari, W. H. Hartt, G. Em Karniadakis, and S. Jamali, "Data-driven physics-informed constitutive metamodeling of complex fluids: a multifidelity neural network (mfnn) framework," *Journal of Rheology*, vol. 65, no. 2, pp. 179–198, 2021.

[9] Y. Mazzi, H. Ben Sassi, A. Gaga, and F. Errahimi, "State of charge estimation of an electric vehicle's battery using tiny neural network embedded on small microcontroller units," *International Journal of Energy Research*, vol. 46, no. 6, pp. 8102–8119, 2022.

[10] C. Yilmaz and I. Koyuncu, "Thermoeconomic modeling and artificial neural network optimization of afyon geothermal power plant," *Renewable Energy*, vol. 163, no. 6, pp. 1166–1181, 2021.

[11] N. Sarada and K. T. Rao, "A neural network architecture using separable neural networks for the identification of "pneumonia" in digital chest radiographs," *International Journal of E-Collaboration*, vol. 17, no. 1, pp. 89–100, 2021.

[12] M. Mcmillan, E. Haber, B. Peters, and J. Fohring, "Mineral prospectivity mapping using a vnet convolutional neural network," *The Leading Edge*, vol. 40, no. 2, pp. 99–105, 2021.

[13] X. Ma, J. Zhou, X. Zhang, and Q. Zhou, "Development of a robotic catheter manipulation system based on BP neural network PID controller," *Applied Bionics and Biomechanics*, vol. 2020, Article ID 8870106, 11 pages, 2020.

[14] B. Zhang, J. Song, S. Zhao, H. Jiang, J. Wei, and Y. Wang, "Prediction of yarn strength based on an expert weighted neural network optimized by particle swarm optimization," *Textile Research Journal*, vol. 91, no. 23-24, pp. 2911–2924, 2021.

[15] C. Fowler, S. An, B. Zheng et al., "Deep neural network inverse-design for long wave infrared hyperspectral imaging," *Applied Computational Electromagnetics Society*, vol. 35, no. 11, pp. 1336-1337, 2021.

[16] J. Huang, W. Sun, and L. Huang, "Joint structure and parameter optimization of multiobjective sparse neural network," *Neural Computation*, vol. 33, no. 4, pp. 1113–1143, 2021.

[17] Q. Liu, W. Zhang, M. W. Bhatt, and A. Kumar, "Seismic nonlinear vibration control algorithm for high-rise buildings," *Nonlinear Engineering*, vol. 10, no. 1, pp. 574–582, 2021.

[18] Z. Huang and S. Li, "Reactivation of learned reward association reduces retroactive interference from new reward learning," *Journal of Experimental Psychology Learning Memory and Cognition*, vol. 48, no. 2, pp. 213–225, 2022.

[19] X. Liu, J. Liu, J. Chen, F. Zhong, and C. Ma, "Study on treatment of printing and dyeing waste gas in the atmosphere with CeMn/GF catalyst," *Arabian Journal of Geosciences*, vol. 14, no. 8, pp. 737–746, 2021.

[20] D. Selva, B. Nagaraj, D. Pelusi, R. Arunkumar, and A. Nair, "Intelligent network intrusion prevention feature collection and classification algorithms," *Algorithms*, vol. 14, no. 8, p. 224, 2021.

[21] R. Huang and X. Yang, "Analysis and research hotspots of ceramic materials in textile application," *Journal of Ceramic Processing Research*, vol. 23, no. 3, pp. 312–319, 2022.